

Available at www.sciencedirect.comjournal homepage: www.elsevier.com/locate/he

Early deuteration steps of Pd- and Ta/Pd- catalyzed Mg₇₀Al₃₀ thin films observed at room temperature

Christopher Harrower^{a,b}, Eric Poirier^c, Helmut Fritzsche^{c,*}, Peter Kalisvaart^{a,b},
Sushil Satija^d, Bulent Akgun^{d,e}, David Mitlin^{a,b}

^aChemical and Materials Engineering, University of Alberta, Alberta T6G 2V4, Canada

^bNational Research Council Canada, National Institute for Nanotechnology, Edmonton, Alberta T6G 2M9, Canada

^cNational Research Council Canada, SIMS, Canadian Neutron Beam Centre, Chalk River, Ontario K0J 1J0, Canada

^dNational Institute of Standards and Technology, Center for Neutron Research, Gaithersburg, MD 20899, USA

^eDepartment of Materials Science and Engineering, University of Maryland, College Park, MD 20742, USA

ARTICLE INFO

Article history:

Received 2 March 2010

Received in revised form

12 May 2010

Accepted 1 August 2010

Available online 1 September 2010

Keywords:

Hydrogen storage

Metal hydride

Catalyst

Thin film

Neutron reflectometry

ABSTRACT

Deuterium absorption in Mg₇₀Al₃₀ thin films coated with a Pd layer and a Ta/Pd bilayer were investigated using in situ neutron reflectometry at room temperature and deuterium pressures up to 1.3 bar. The approach used provides a detailed profile, at the nanoscale, of the deuterium content inside the specific layers that constitute the films. It is found that Mg₇₀Al₃₀ can store up to 5 wt.% under these mild conditions following a two-step mechanism. The latter involves the deuteration of the top and bottom catalyst layers first, followed by the main Mg₇₀Al₃₀ layer. The presence of deuterium throughout the films in the early absorption stages evidences atomic deuterium spillover from the catalyst layers. The addition of a Ta layer between the Pd and Mg₇₀Al₃₀ was found to allow observable absorption at a pressure 10 times lower than on the Ta-free sample, without affecting the storage capacity. Our measurements imply that this improvement in kinetics is due to a lowering of the nucleation barrier for the formation of the hydride phase in the Mg₇₀Al₃₀ layer.

Crown Copyright © 2010 Published by Elsevier Ltd on behalf of Professor T. Nejat Veziroglu. All rights reserved.

1. Introduction

Magnesium and its alloys are amongst the most promising candidates for solid-state hydrogen storage applications owing to their high hydrogen capacity of 7.6 wt.% and their low cost [1]. The main drawback seen by Mg is the high temperature, on the order of 300 °C typically required to obtain fast hydrogen absorption and desorption kinetics. This temperature is deemed too high for mobile applications and its reduction by means of catalysts addition and nanostructuring is now widely investigated [2–5]. The

hydrogenation of magnesium is commonly described with two models: (i) a nucleation and growth model where the hydride grains may impinge before the whole Mg particle is hydrided and (ii) the three-dimensional diffusion-controlled shrinking-core model, where a continuous layer of hydride forms immediately on the surface and reduces significantly the hydride formation because of the reduced diffusion rate through the hydride layer [6]. The addition of catalysts may alter significantly the hydriding kinetics by lowering hydrogen dissociation and diffusion barriers [7]. To investigate these effects, thin films are very interesting model systems which

* Corresponding author.

allow incorporation of catalysts in a well controlled manner at the nanoscale. Recent studies of hydrogen absorption in Mg thin films capped with a Pd catalyst layer showed that absorption is possible near ambient temperature and pressure [8]. A theoretical study suggested room temperature absorption on such systems may be promoted by a spillover mechanism from the Pd into the Mg alloy phase [9]. Nevertheless, a detailed representation of the hydrogen absorption mechanism in such systems lacks of experimental measurements at the nanoscale. Neutron reflectivity (NR) has proved to constitute a powerful tool for profiling the hydrogen or deuterium content with nanometer resolution in the distinct layers that constitute films [10,11]. It has recently been shown using NR that the use of a Ta/Pd bilayer catalyst on a $\text{Mg}_{70}\text{Al}_{30}$ film layer improves its kinetics properties [12], leading to hydrogen desorption at 100 °C compared to 170 °C for a single Pd layer [13]. The addition of Ta did not lead to a diminution of the gravimetric hydrogen storage capacity of the film, a somehow expected consequence of catalytic enhancement. The effect of the Ta catalyst layer on the absorption properties at room temperature remains, however, an open question. In order to investigate the absorption mechanism and the effectiveness of a Ta/Pd bilayer as a catalyst for room temperature absorption, we used NR to observe and compare the deuteration mechanism of two $\text{Mg}_{70}\text{Al}_{30}$ thin films with a Pd-layer and Ta/Pd-bilayer catalyst, respectively. We chose the $\text{Mg}_{70}\text{Al}_{30}$ alloy because it is the composition with the optimum desorption properties as was determined in previous studies [13,14]. The measurements were performed in situ at distinct stages of the absorption process, under quasi-equilibrium conditions, from the early deuteration steps in catalyst layers up to the full saturation of the samples. The concentration profiles thus obtained offer new insights in how absorption proceeds on such metal systems, and how the use of certain catalysts may lead to improved materials.

2. Experimental

To study the influence of a Ta catalyst layer, we compare a 50-nm thick $\text{Mg}_{70}\text{Al}_{30}$ film capped with a 10-nm thick Pd catalyst layer with a 50-nm thick $\text{Mg}_{70}\text{Al}_{30}$ film capped with a 5-nm/5-nm thick Ta/Pd bilayer. The thin film samples used in this study were fabricated by co-sputtering onto a native oxide (100) silicon wafer in a confocal sputtering chamber (Orion 5 instrument from AJA International) [15] operating at an Ar (purity 99.999% pure) pressure of 5×10^{-3} mbar which had been previously evacuated to a pressure less than 3×10^{-8} mbar. First a 10-nm Ta buffer layer was deposited onto the wafer and, without interruption, a 50-nm $\text{Mg}_{70}\text{Al}_{30}$ layer was co-sputtered followed by either a 10-nm Pd layer or a 5-nm Ta/5-nm Pd bilayer. The sample structure is depicted in Fig. 1. The investigated films have the same structure as previously reported [12,16], i.e., no intermetallics in the as-prepared state and the first absorption cycle. The microstructure consists of a supersaturated solid solution of Al in Mg with a strong texture along the surface normal, i.e., Mg (002) is parallel to Si(100), but we do not observe a single crystal growth. The HCP structure of the Mg is maintained with a contracted lattice parameter due to Al in solution. The

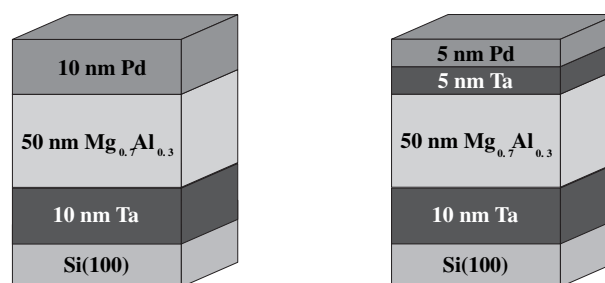


Fig. 1 – Illustration of the structure of the film with the single Pd catalyst layer (left) and the Ta/Pd catalyst bilayer (right).

lattice parameter follows a Vegard's law wherein the lattice contracts proportional to the Al concentration in the Mg. A contracted lattice is only noticed in the as-prepared material and is not noticed in the material once hydride – the Al precipitates out of MgH_2 and remains as a precipitate.

Neutron Reflectometry (NR) experiments were conducted on the NG7 reflectometer at the National Institute of Standards and Technology, Center for Neutron Research, Gaithersburg MD, USA. This instrument has a resolution of $\Delta q/q = 4\%$ using a 4.75-Å wavelength. The deuterium absorption was performed in situ, using an aluminum sample cell, at room temperature from a deuterium pressure of $\sim 10^{-4}$ mbar up to 1.3 bar using ultra high purity deuterium (99.999%). The reflectivity curves were measured at grazing incidence, in specular geometry as a function of the incident angle θ . In this configuration, the neutron interaction with the films is reduced to a one-dimensional problem that can be described with a neutron index of refraction analogous to optical reflectivity. The neutron index of refraction depends on the strength of the interaction of neutrons with a specific isotope in the film and can be represented by [17]:

$$n^2 = 1 - \frac{\lambda^2}{\pi} N_j b_j \quad (1)$$

where λ is the neutron wavelength, N_j is the number density, b_j is the coherent nuclear scattering length and the product $N_j b_j = S$ is the scattering length density (SLD) of the layer. The SLD of each layer depends on their elements and their isotopes in the sample [18,19]. Deuterium is used because of its large coherent scattering length, which leads to a dramatic increase in the layers' SLD, creating a strong contrast in the SLD of the deuterated layers with respect to the as-prepared material. Total reflection of neutrons occurs up to a critical scattering vector q_c calculated as [17]:

$$q_c = \frac{4\pi}{\lambda} \sin \theta_c = 4\sqrt{\pi N b} \quad (2)$$

The evolution of q_c upon deuteration is a good indicator of the average deuterium content in the film. Short measurements showing the movement of the critical edge upon deuteration were helpful in monitoring the absorption kinetics. Typically, the measurements over the $q = 0 - 0.1 \text{ \AA}^{-1}$ range were considered as quasi-equilibrium when the kinetics was sufficiently slow, i.e., with the critical edge, or the full NR curve showing no major changes over a 1–2 h measurement

time. Some measurements not satisfying this condition could not be fitted and were rejected.

The reflectivity curves were modeled using Parratt's recursive algorithm, which involves a slab model and yields the SLD as a function of depth [20]. Interfacial roughness is accounted for in this approach. From the modeled SLD profiles, the corresponding atomic deuterium concentration C_D in each layer can be approximated by taking into account film expansion according to the relationship [11]:

$$C_D \cong \left[\frac{S_{M+D}}{S_{M(p=0)}} \frac{t_{M+D}}{t_M} - 1 \right] \frac{b_M}{b_D} \quad (3)$$

where S_{M+D} is the SLD of the deuterium-charged layer, $S_{M(p=0)}$ is the SLD of the metal in absence of deuterium, t_{M+D} and t_M are the corresponding thicknesses, and b_M and b_D are the coherent scattering lengths of the metal and deuterium, respectively. It is important to mention that the NR technique measures the deuterium/hydrogen content in the layers and cannot discriminate between the existence of a metal hydride and a solid solution.

3. Results

In Fig. 2 the measured and calculated reflectivity curves (open circles and solid line, respectively) of the Ta/Mg₇₀Al₃₀/Pd film structure are shown as a function of the scattering vector q . The visible oscillations, referred to as Kiessig fringes, are associated with a characteristic thickness of the film. The calculated SLD profiles, i.e., the SLD as a function of z , the direction parallel to the surface normal of the film, are displayed in the insets. These insets provide a real space representation of the film. The as-prepared sample measured in air (Fig. 2a) clearly indicates the as-synthesized structure as a 10-nm Pd, 50-nm Mg₇₀Al₃₀, and 10-nm Ta buffer layer on top of a Si(100) substrate. It is worth noting the SLDs of the different layers ($4.0 \times 10^{-6} \text{ \AA}^{-2}$, $2.4 \times 10^{-6} \text{ \AA}^{-2}$, and $3.8 \times 10^{-6} \text{ \AA}^{-2}$, respectively) are within 10% of the expected individual bulk values that further supports the measurement and calculation procedure. The sharp delimitation of the distinct layers indicates that there is very little interfacial roughness between each layer. Subsequently, deuterium was introduced into the sample cell and reflectometry measurements taken. As a consequence of the large coherent scattering length of deuterium [19], the SLD of the absorbing layer increases, as seen in Fig. 2. In particular, at a pressure of 20 mbar (Fig. 2b), it is striking that little, or no deuterium, is present in the Mg₇₀Al₃₀ layer (SLD = $2.4 \times 10^{-6} \text{ \AA}^{-2}$, as initially), while the SLD of the surrounding Pd and Ta is $\sim 5.0 \times 10^{-6} \text{ \AA}^{-2}$ and $\sim 4.6 \times 10^{-6} \text{ \AA}^{-2}$, respectively, corresponding to a deuterium to metal ratio of $D/M=0.2$. After a further deuterium pressure increase to 1.3 bar the SLD of the Pd and Ta increase further to $6.5 \times 10^{-6} \text{ \AA}^{-2}$ and $5 \times 10^{-6} \text{ \AA}^{-2}$, corresponding to $D/M=0.46$ and $D/M=0.2$, respectively.

At a deuterium pressure of 1.3 bar (Fig. 2c) there is a slight increase in the SLD of the Mg₇₀Al₃₀ layer corresponding to $D/M=0.12$. This deuterium concentration in the Mg₇₀Al₃₀ layer is consistent with a solid solution with no rearrangement (phase transformation) of the Mg₇₀Al₃₀. After immersion in a 1.3 bar deuterium for 10+ hours (Fig. 2d), the Mg₇₀Al₃₀ layer SLD saturates at $5.5 \times 10^{-6} \text{ \AA}^{-2}$ and expands

by $\sim 23\%$, corresponding to $D/M=1.35$. This deuterium concentration in the Mg layer is consistent with MgD₂ formation (a maximum of $D/M=1.4$ is possible in our Mg₇₀Al₃₀ layer), an observation previously observed on similar samples [16]. This large amount of deuterium absorption in the Mg₇₀Al₃₀ layer can also be easily deduced from the shift of the critical edge to larger q , as described in equation (2). Noticeably, a small concentration gradient is visible in the deuterated Mg₇₀Al₃₀ phase (see Fig. 3), and small interfacial layers between Mg₇₀Al₃₀ and the Ta and Pd layers remain free of deuterium in these conditions.

In Fig. 4 the measured and calculated reflectivity curves (open circles and solid line, respectively) of the Ta/Mg₇₀Al₃₀/Ta/Pd film are shown as a function of the scattering vector q ,

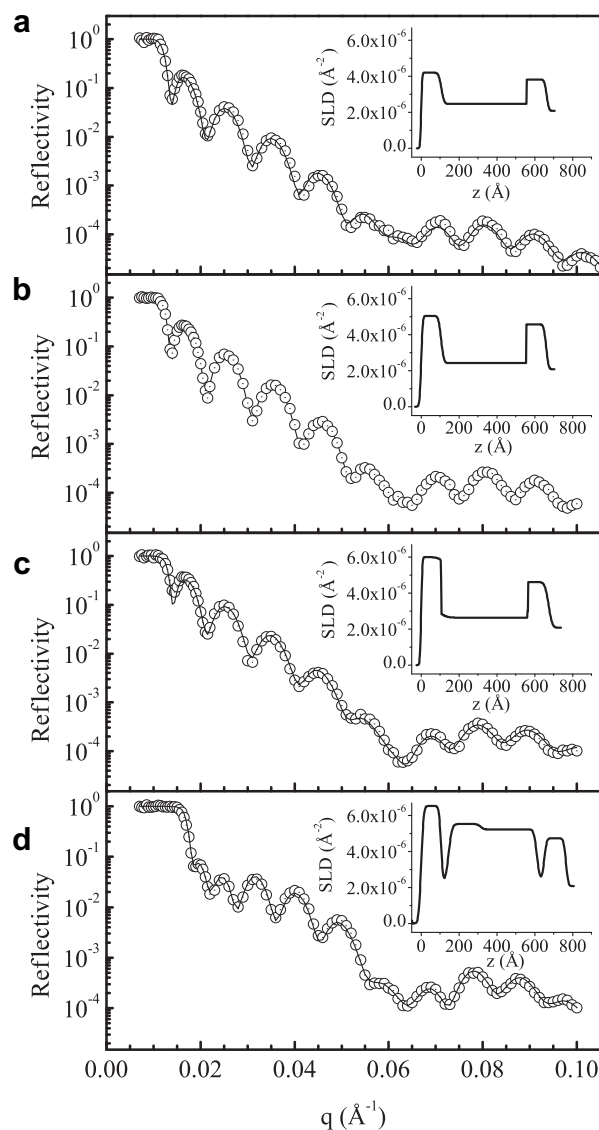


Fig. 2 – Reflectivity curve of Si/Ta/Mg₇₀Al₃₀/Pd: (a) as prepared, (b) at a deuterium pressure of 20 mbar, (c) at a deuterium pressure of 1.3 bar for 1 h, (d) at a deuterium pressure of 1.3 bar for 10+ hours. The open circles represent the measured data with errors always smaller than the circles, the solid lines represent a fit as described in the text.

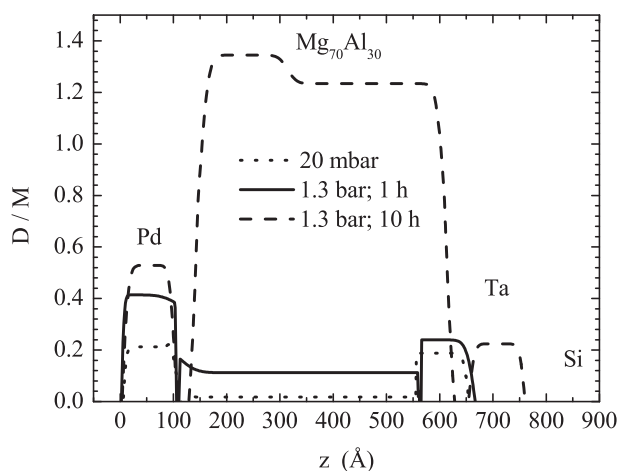


Fig. 3 – Overview of the deuterium concentration profile in D/M during the different deuteration stages in $\text{Si/Ta/Mg}_{70}\text{Al}_{30}/\text{Pd}$: at a deuterium pressure of 20 mbar after 1 h (dotted curve); at 1.3 bar after 1 h (solid curve); at 1.3 bar after 10+ hours (dashed curve).

similar to measurements performed on the sample with the single Pd catalyst layer. The SLD profile of the as-prepared sample (Fig. 4a) clearly indicates the structure as 5 nm Pd, 5 nm Ta, 50 nm $\text{Mg}_{70}\text{Al}_{30}$, and 10 nm Ta on top of a Si(100) substrate. This SLD profile is in accordance with expected SLD values from bulk SLD values and deposition parameters. Following the introduction of D_2 up to 6.5 mbar (Fig. 4b), it is visible that both the top and bottom layers contain deuterium, while the $\text{Mg}_{70}\text{Al}_{30}$ phase has little, or no, deuterium. In that respect, absorption in this sample seems to follow the same early filling steps as observed in the Pd-capped sample, however, the subsequent deuterium absorption of the $\text{Mg}_{70}\text{Al}_{30}$ phase (Fig. 4c) occurs at a much lower pressure, about ~ 140 mbar. Also, at this pressure, the deuterium concentration profile in the $\text{Mg}_{70}\text{Al}_{30}$ layer exhibits a significant gradient as illustrated by a varying SLD profile (Fig. 4c) in the film, corresponding to $D/M = 1.27$ at the top Ta layer to 0.73 at the bottom Ta layer (Fig. 5). This gradient may be due, in part, to the low applied pressure which results in a low driving force for diffusion through the $\text{Mg}_{70}\text{Al}_{30}$ layer. After several hours at 140 mbar the SLD profile shows a reduced gradient with an average SLD of about $5.5 \times 10^{-6} \text{ \AA}^{-2}$ in the $\text{Mg}_{70}\text{Al}_{30}$, corresponding to $D/M = 1.35$. Also, the thickness of the $\text{Mg}_{70}\text{Al}_{30}$, from the as-prepared material to the final absorption, expanded by $\sim 23\%$, a value comparable to that observed in the Pd-capped film. The SLD of the top Pd and Ta layers are $4.7 \times 10^{-6} \text{ \AA}^{-2}$ and $6.1 \times 10^{-6} \text{ \AA}^{-2}$, respectively, while the bottom Ta layer has a reduced SLD (compared to the catalyst layer) of $4.7 \times 10^{-6} \text{ \AA}^{-2}$, corresponding to $D/M = 0.2, 0.6$, and 0.2 in the top Pd, Ta, and bottom Ta layer, respectively.

4. Discussion

The present observation of the early stages of deuterium absorption in the films illustrates that the absorption

mechanism of deuterium involves the absorption in the top and bottom layers, followed by absorption in the $\text{Mg}_{70}\text{Al}_{30}$ layer. The early presence of D throughout the film in these conditions evidences the occurrence of a spillover mechanism associated with a significant lowering of dissociation and diffusion barriers due to the catalyst layers [9]. Therefore, our measurements confirm that the dissociation barrier of D_2 on Pd is essentially negligible [21] and the diffusion is fast through Pd and Mg layers on the nanometer scale [22]. On the other hand, the late formation of MgD_2 is surprising since it is much more thermodynamically favorable compared to Pd and Ta hydrides, i.e., the enthalpies of formation for these hydrides are $\Delta H_{\text{Mg}} = -75 \text{ kJ/mol}$ [23], $\Delta H_{\text{Pd}} = -35 \text{ kJ/mol}$ [24] and $\Delta H_{\text{Ta}} = -70 \text{ kJ/mol}$ [25]. In fact, from these equilibrium

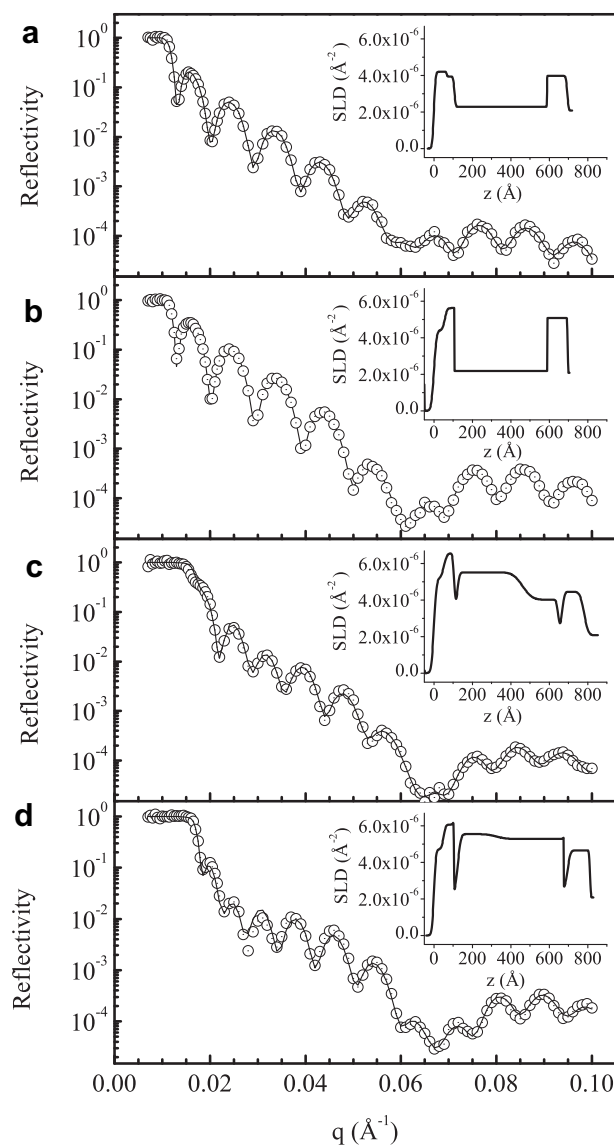


Fig. 4 – Reflectivity curve of $\text{Si/Ta/Mg}_{70}\text{Al}_{30}/\text{Ta/Pd}$: (a) as prepared, (b) at a 6.5 mbar deuterium pressure for 1 h, (c) at a deuterium pressure of 140 mbar after 1 h, (d) at a deuterium pressure of 140 mbar at saturation after 10+ hours. The open circles represent the measured data with errors always smaller than the circles, the solid lines represent a fit as described in the text.

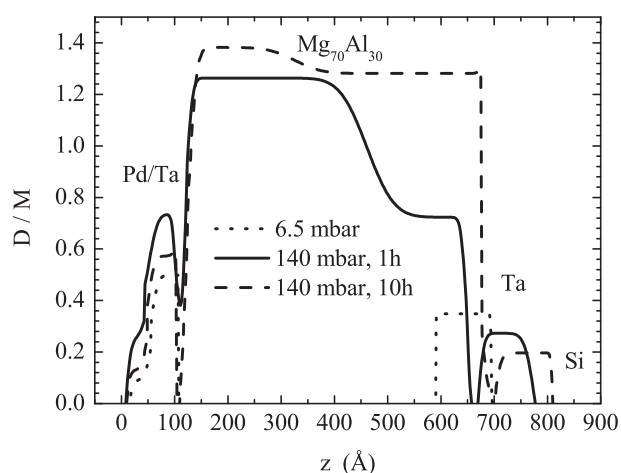


Fig. 5 – Overview of the deuterium concentration profile in D/M during the different deuterium absorption stages in Si/Ta/ $Mg_{70}Al_{30}$ /Ta/Pd: at a 6.5 mbar deuterium pressure for 1 h (dotted curve); at a deuterium pressure of 140 mbar for 1 h (solid curve); at saturation after 10+ hours at 140 mbar (dashed curve).

thermodynamics considerations, it appears that the initial pressure is sufficiently high for the formation of MgD_2 , i.e., the plateau pressure for bulk Mg is 1×10^{-3} mbar. This leaves the deuterium absorption hindered mainly by a phase transformation (Mg to MgH_2) nucleation barrier. The latter may include a volume expansion barrier, as well as a phase interface barrier [3]. In the present case, the volume expansion work required to form the new phase might represent the main contribution. This is supported by a large $\sim 23\%$ expansion of the $Mg_{70}Al_{30}$ layer observed upon absorption, a value much larger than those of the easily deuterated Pd and Ta layers. The latter expand by about 2% and 6%, respectively. The reduced pressure used to absorb deuterium into $Mg_{70}Al_{30}$ /Ta/Pd may be due to a better elastic disconnection [26] between the $Mg_{70}Al_{30}$ and the Ta/Pd bilayer leading to a reduction of the nucleation barrier. This better elastic disconnection cannot be attributed to less interdiffusion of the $Mg_{70}Al_{30}$ /Ta compared to $Mg_{70}Al_{30}$ /Pd because our samples clearly show sharp $Mg_{70}Al_{30}$ /Ta and $Mg_{70}Al_{30}$ /Pd interfaces with an rms roughness of about 0.5 nm, as deduced from the NR curves shown in Figs. 2a and 4a. Moreover, it should be noted that the reduced required pressure to deuterate the $Mg_{70}Al_{30}$ /Ta/Pd film cannot be associated with thermodynamic changes due to different compositions and structure as the starting SLD (composition) and thicknesses of the $Mg_{70}Al_{30}$ layers in each case are similar.

The observed large deuterium concentration gradient in the $Mg_{70}Al_{30}$ films during the absorption process (see Fig. 4c) might be due to the MgD_2 acting as a diffusion barrier at this low pressure (1 bar) and room temperature. In our previous studies on $Mg_{70}Al_{30}$ films [12,13] we charged the samples at 40 bar and $125^\circ C$ and always observed a homogeneous hydrogen concentration. The remaining small MgD_2 gradient at saturation might be due to a preferred segregation of MgD_2 at one interface as was observed earlier in $Mg_{70}Al_{30}$ films [27]. The measured D/M ratio of 1.35 at saturation in the $Mg_{70}Al_{30}$ layer is

a little bit higher than previously determined on similar $Mg_{70}Al_{30}$ films [12,13] because the experiments reported here were done in situ in D_2 atmosphere, whereas the previous NR experiments had been performed in an Ar atmosphere after an ex situ hydrogen absorption. A slight hydrogen desorption at room temperature [12] is the cause for the smaller hydrogen content in these ex situ charged samples.

The deuterium concentration in the Pd ($D/M = 0.4$) and Ta ($D/M = 0.2$) layer at saturation is lower than values for bulk hydrides ($H/M = 0.7-0.8$). This is in agreement with the Pd thickness dependence of the thermodynamic properties as determined by electrochemical measurements [28] which show a narrowing of the miscibility gap for decreasing Pd film thickness. The same narrowing of the miscibility gap, accompanied by a reduced hydrogen storage capacity was observed in Pd nano-particles with 8–12 nm grain size [29].

From the SLD curves we can deduce the existence of a region (2–4 nm) devoid of deuterium at the $Mg_{70}Al_{30}$ /Pd and $Mg_{70}Al_{30}$ /Ta interfaces. The presence of such a hydrogen depletion zone is consistent with previous investigations of a Ti/Mg/Pd stack by Baldi et al. [26,30] who found that an approximate 6 nm of the Mg layer did not hydrogenate and assumed that it is due to Mg–Pd alloying. As mentioned above, the present samples clearly show sharp interfaces (see Figs. 2a and 4a), as well as consistency in the shape and thickness of the Pd and Ta layers upon deuterium absorption. Therefore, we can conclude alloying is not the cause of the observed depletion zones in our samples. In a previous NR study we clearly showed that Mg–Pd interdiffusion occurs in MgAl thin films, but only at elevated temperatures ($\sim 200^\circ C$) [31]. Therefore, the observed interfacial regions devoid of deuterium are likely due to elastic constraints between layers hindering Mg expansion and resulting in a higher required absorption pressure in that region [32,33].

5. Conclusions

In conclusion, the present study provides new insights into the early stages of hydrogen absorption mechanism in nanoscale films at room temperature. In particular these measurements suggest that hydrogenation of $Mg_{70}Al_{30}$ thin films with different catalyst layers can occur through a two-step mechanism. One of the mechanisms likely mirrors the peculiarity of the interfaces in which elastic constraints at the interfaces may affect the nucleation barrier for the formation of hydrides. The addition of a Ta layer in the top catalyst was found to improve the sorption kinetics significantly, leading to a reduction of the required D_2 pressure by a factor 10 without significantly reducing the hydrogen storage capacity. Furthermore, it was observed that non-absorbing regions developed between the catalyst (either Pd or Ta/Pd catalyst) and the $Mg_{70}Al_{30}$ layer. These regions are attributed to interfacial stress, as alloy formation is not consistent with the observed results. Finally, the deuterium absorption in the $Mg_{70}Al_{30}$ phase reaches $D/M = 1.35$ or the equivalent of about 5 wt.% H, a considerable value under the mild present conditions. These findings clearly illustrate the absorption process and a degree of optimization that can be achieved with a nanoscale model system under highly controlled conditions.

Acknowledgement

We thank Michael Gharghoury (NRC, CNBC) for his valuable comments on our manuscript.

REFERENCES

- [1] Schlapbach L, Züttel A. Hydrogen-storage materials for mobile applications. *Nature* 2001;414:353.
- [2] Sakintuna B, Lamari-Darkrim F, Hirscher M. Metal hydride materials for solid hydrogen storage: a review. *Int J Hydrogen Energy* 2007;32:1121.
- [3] Bérubé V, Radtke G, Dresselhaus M, Chen G. Size effects on the hydrogen storage properties of nanostructured metal hydrides: a review. *Int J Energy Res* 2007;31:637.
- [4] Yonkeu AL, Swainson IP, Dufour J, Huot J. Kinetic investigation of the catalytic effect of a body centered cubic-alloy TiV₁.1Mn_{0.9} (BCC) on hydriding/dehydriding properties of magnesium. *J Alloys Compd* 2008;460:559.
- [5] Tan XH, Harrower CT, Amirkhiz BS, Mitlin D. Nano-scale bilayer Pd/Ta, Pd/Nb, Pd, Ti and Pd/Fe catalysts for hydrogen sorption in magnesium thin films. *Int J Hydrogen Energy* 2009;23:7741.
- [6] Tien HY, Tanniru M, Wu CY, Ebrahimi F. Effect of hydride nucleation rate on the hydrogen capacity of Mg. *Int J Hydrogen Energy* 2009;34:6343.
- [7] Banerjee S, Pillai CGS, Majumder C. Dissociation and diffusion of hydrogen on the Mg(0001) surface: catalytic effect of V and Ni double substitution. *J Phys Chem C* 2009;113:10574.
- [8] Shalaan E, Schmitt H. Mg nanoparticle switchable mirror films with improved absorption–desorption kinetics. *Surf Sci* 2006;600:3650.
- [9] Du AJ, Smith SC, Yao XD, Lu GQ. Hydrogen spillover mechanism on a Pd-doped Mg surface as revealed by ab initio density functional calculation. *J Am Chem Soc* 2007;129:10201.
- [10] Munter AE, Heuser BJ, Ruckman MW. In situ neutron reflectometry measurements of hydrogen and deuterium absorption in a Pd/Nb/Pd layered film. *Phys Rev B* 1997;55:14035.
- [11] Rehm C, Fritzsche H, Maletta H, Klose F. Hydrogen concentration and its relation to interplanar spacing and layer thickness of 1000-Å Nb(110) films during in situ hydrogen charging experiments. *Phys Rev B* 1999;59:3142.
- [12] Fritzsche H, Ophus C, Harrower CT, Lubner E, Mitlin D. Low temperature hydrogen desorption in MgAl thin films achieved by using a nanoscale Ta/Pd bilayer catalyst. *Appl Phys Lett* 2009;94:241901.
- [13] Fritzsche H, Saoudi M, Haagsma J, Ophus C, Lubner E, Harrower CT, et al. Neutron reflectometry study of hydrogen desorption in destabilized MgAl alloy thin films. *Appl Phys Lett* 2008;92:121917.
- [14] H Fritzsche, E Poirier, J Haagsma, C Ophus, E Lubner, CT Harrower, et al. A systematic neutron reflectometry study on hydrogen absorption in thin Mg_{1-x}Al_x alloy films. *Can J Phys* 88, in press.
- [15] Commercial materials, instruments and equipment are identified in this paper in order to specify the experimental procedure as completely as possible. In no case does such identification imply a recommendation or endorsement by NIST nor does it imply that the materials, instruments, or equipment identified are necessarily best available for the purpose.
- [16] Kalisvaart WP, Harrower CT, Haagsma J, Zahiri B, Lubner EJ, Ophus C, et al. Hydrogen storage in binary and ternary Mg-based alloys: a comprehensive experimental study. *Int J Hydrogen Energy* 2010;35:2091.
- [17] Zhou XL, Chen SH. Theoretical foundation of X-ray and neutron reflectometry. *Phys Reports* 1995;257:223.
- [18] Sears VF. Neutron scattering lengths and cross sections. *Neutron News* 1992;3:26.
- [19] Available from: <www.ncnr.nist.gov/resources/n-lengths>.
- [20] Parratt LG. Surface studies of solids by total reflection of X-rays. *Phys Rev* 1954;95:359.
- [21] Dong W, Hafner J. H₂ dissociative adsorption on Pd(111). *Phys Rev B* 1997;56:15396.
- [22] Kirchheim R. Solubility and diffusivity of hydrogen in complex materials. *Physica Scripta* 2001;T94:58.
- [23] Bogdanovic B, Boehmhammel K, Christ B, Reiser A, Schlichte K, Vehlen R, et al. Thermodynamic investigation of the magnesium–hydrogen system. *J Alloys Compd* 1999;282:84.
- [24] Pivak Y, Gremaud R, Gross K, Gonzalez-Silveira M, Walton A, Book D, et al. Effect of the substrate on the thermodynamic properties of PdH_x films studied by hydrogenography. *Scripta Materialia* 2009;60:348.
- [25] San-Martin A, Manchester FD. The H–Ta (Hydrogen Tantalum) system. *J Phase Equilibria* 1991;12:337.
- [26] Baldi A, Gonzalez-Silveira M, Palmisano V, Dam B, Griessen R. Destabilization of the Mg–H system through elastic constraints. *Phys Rev Lett* 2009;102:226102.
- [27] Gremaud R, Borgschulte A, Chacon C, Van Mechelen JLM, Schreuders H, Züttel A, et al. Structural and optical properties of Mg_xAl_{1-x}H_y gradient thin films: a combinatorial approach. *Appl Phys A* 2006;84:77.
- [28] Vermeulen P, Ledovskikh A, Danilov D, Notten PHL. The impact of the layer thickness on the thermodynamic properties of Pd hydride thin film electrodes. *J Phys Chem B* 2006;110:20350.
- [29] Pundt A, Kirchheim R. Hydrogen in metals: microstructural aspects. *Annu Rev Mater Res* 2006;36:555.
- [30] Baldi A, Palmisano V, Gonzalez-Silveira M, Pivak Y, Slaman M, Schreuders H, et al. Quasi-free Mg–H thin films. *Appl Phys Lett* 2009;95:071903.
- [31] Fritzsche H, Saoudi M, Haagsma J, Ophus C, Harrower CT, Mitlin D. Structural changes of thin MgAl films during hydrogen desorption. *Nucl Instr Meth A* 2009;600:301.
- [32] Lufitano J, Sofronis P, Birnbaum HK. Elastoplastically accommodated hydride formation and embrittlement. *J Mech Phys Solids* 1998;46:1497.
- [33] Zoltowski P. Effects of self-induced mechanical stress in hydrogen sorption by metals, by EIS. *Electrochimica Acta* 1999;44:4415.